European Journal of Medicinal Chemistry 46 (2011) 2652–2661

Contents lists available at ScienceDirect

European Journal of Medicinal Chemistry

journal homepage: http://www.elsevier.com/locate/ejmech

Original article

In vitro and *in vivo* anticancer activity evaluation of ursolic acid derivatives

Jing-Wei Shao*, Yong-Chao Dai, Jin-Ping Xue, Ji-Chuang Wang, Feng-Ping Lin, Yang-Hao Guo

Chemistry and Chemical Engineering College of Fuzhou University, #2, Xueyuan Road, Fuzhou 350108, PR China

ARTICLE INFO

Article history:
Received 18 November 2010
Received in revised form
15 March 2011
Accepted 22 March 2011
Available online 3 April 2011

Keywords:
Ursolic acid derivatives
Synthesis
Cytotoxicity
Anticancer activity
Apoptosis

ABSTRACT

Twenty-three ursolic acid (1) derivatives **2**–**24** (ten novel compounds **8**–**10**, **14**–**17** and **22**–**24**) modified at the C-3 and the C-28 positions were synthesized, and their structures were confirmed by IR, ^{1}H NMR, MS, and elemental analysis. The single crystals of compounds **15** and **17** were obtained. The cytotoxic activity of the derivatives was evaluated against HepG2, BGC-823, SH-SY5Y, HeLa and HELF cells by the MTT assay. The induction of apoptosis and affects on the cell cycle distribution with compound **14** were assessed by fluorescence microscopy, flow cytometry and the activity of caspase-3 in HepG2 cells. Compounds **14**–**17** had more significant antiproliferative ability against the four cancer cell lines and low cytotoxicity to human embryonic lung fibroblast cells (HELF). Compounds **11, 14**–**16, 21** and **23** were particularly active against HepG2 cell growth. Compound **14** was selected to investigate cell apoptosis and cell cycle distribution. Flow cytometric analysis and morphologic changes of the cell exhibited that treatment of HepG2 cells with compound **14** led to cell apoptosis accompanied by cell cycle arrest at the S phase in a dose-dependent manner. Furthermore, the activity of the caspase-3 enzyme was increased in the treated cells. *In vivo* studies using H22 xenografts in Kunming mice were conducted with compound **14** at doses of 50, 100 and 150 mg/kg body weight. The results revealed that the medium dosage group (100 mg/kg) showed significant anticancer activity (45.6 ± 4.3%) compared to the control group.

1. Introduction

Ursolic acid (UA, 3β-hydroxy-urs-12-en-28-oic acid **1**), a pentacyclic triterpene acid, exists abundantly in the plant kingdom. Ursolic acid and its derivatives have been reported to have interesting bioactivity, including anti-HIV [1], antihepatodamage [2], antimalarial [3], antimicrobial and anti-inflammatory activity [4]. Recent studies have shown that ursolic acid has marked anti-tumor effects and cytotoxic activity toward various types of cancer cell lines *in vitro* [5–7].

As an effective natural anticancer drug, considerable structural modification has been performed on ursolic acid to obtain potential anticancer compounds. Ursolic acid has been treated with different anhydrides in pyridine or tetrahydrofuran to obtain a series of 3-O-acyl derivatives [8,9]. Amino acid was connected to ursolic acid after its 17-COOH was chlorinated with oxalyl chloride [10]. Some derivatives have shown significant cytotoxicity against some tumor cell lines [10,11]. The structure–activity relationship demonstrated that a hydrogen donor group at either position 3 and/or 28 was essential for cytotoxic activity, and a significant improvement in cell growth inhibition was observed when an acetyl group was introduced on the 3-OH, and when amino alkyl groups were introduced at the 17-COOH position.

However, derivatives have not been thoroughly explored for their anti-tumor activity. To search for potentially important anti-tumor drug candidates, study their structure–activity relationships and explore their mechanisms, a series of UA derivatives were synthesized, and their cytotoxic activities were evaluated against human hepatoma cells HepG2, human gastric cancer cells BGC-823, human neuroblastoma cells SH-SY5Y, human cervical carcinoma cells HeLa, and human embryonic lung fibroblast HELF. Investigations of the mechanism and anti-tumor activity *in vivo* were performed on compound **14** and UA.

2. Results and discussion

2.1. Chemistry

Chemical transformations of the active compound were carried out to study the structure–activity relationships.

Ursolic acid (**1**) was acetylated to give 3-O-acetylursolic acid. Treatment of Ursolic acid or 3-O-acetylursolic acid with the bromodiolefine afforded fatty esters **2**–**4** (Scheme 1) or **8**–**10** (Scheme 2),

* Corresponding author. Tel.: +86 13600802402; fax: +86 59187892632.
E-mail addresses: shaojingwei@fzu.edu.cn, sophia8762@yahoo.com.cn (J.-W. Shao).

0223-5234/$ – see front matter © 2011 Elsevier Masson SAS. All rights reserved.
doi:10.1016/j.ejmech.2011.03.050

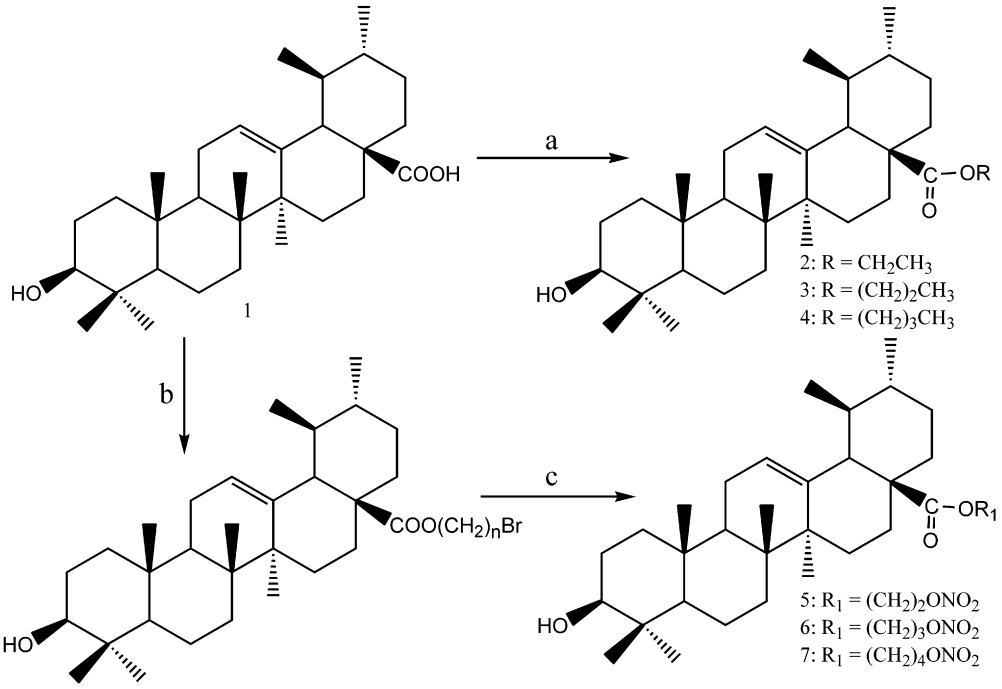

Scheme 1. Synthesis of ester derivatives of ursolic acid. Reagents and conditions: (a) $CH_3(CH_2)_nBr$, K_2CO_3, DMF, r.t.; (b) $Br(CH_2)_nBr$, K_2CO_3, DMF, r.t.; (c) $AgNO_3/CH_3CN$, $COO(CH_2)_nBr$.

respectively. Ursolic acid (**1**) was treated with dibromo-diolefine to obtain intermediate products, which were further reacted with $AgNO_3$ to yield nitrate esters **5**–**7** (Scheme 1). 3-O-acetylursolic acid was treated with oxalyl chloride to give the 28-acylchloride, which was then condensed with the appropriate amino compound (methyl ester of serine, tyrosine, 2-aminoethanol, 2-aminodiethanol, *N*- (2-Hydroxyethyl) piperazine, 1-hydroxyethylethoxypiperazine or 4-piperidineethanol) in the presence of triethylamine to provide compounds **11**–**17** (Scheme 2). Saponification of compounds **11**–**17** gave the corresponding compounds **18**–**24** (Scheme 2). All the new compounds were fully characterized by various spectroscopic methods, including Infrared (IR), ^{1}H NMR, mass spectra (MS) and element analysis. In addition, single crystal of compound **15** and **17** were obtained by layering hexane on a mixture of dichloromethane

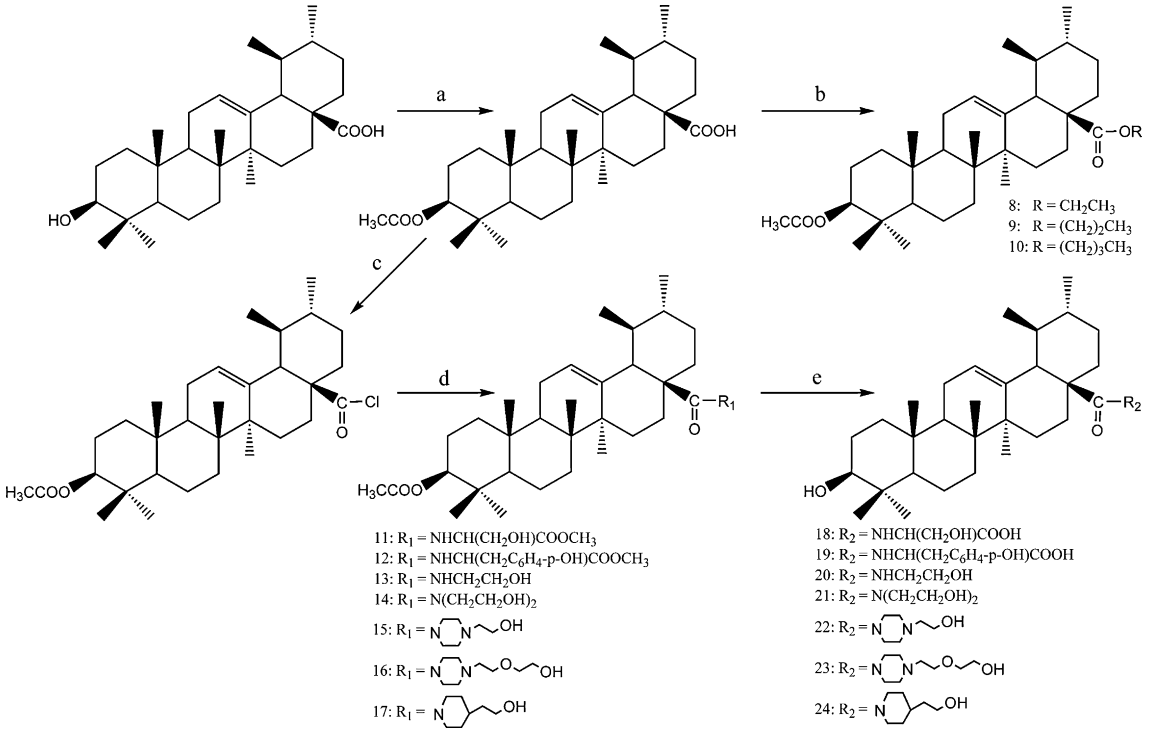

Scheme 2. Synthesis of amides and other ester derivatives of ursolic acid. Reagents and conditions: (a) anhydride/Pyr/DMAP, r.t.; (b) $CH_3(CH_2)_nBr$, K_2CO_3, DMF, r.t.; (c) $(CO)_2Cl$, CH_2Cl_2, r.t.; (d) CH_2Cl_2, Et_3N, HR, r.t.; (e) NaOH, CH_3OH/THF, r.t.

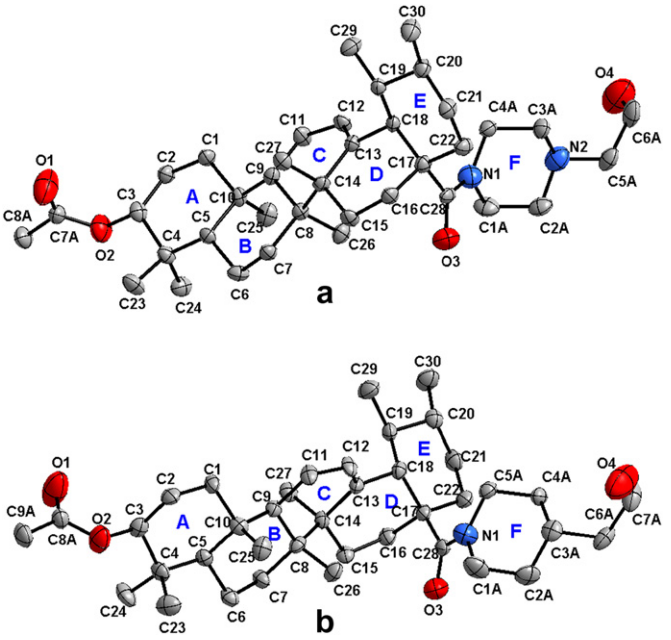

Fig. 1. Molecular structure of compounds. (a) compound 15; (b) compound 17. H atoms have been omitted for clarity.

and methanol. These compounds crystallize in the orthorhombic space group P21 (Fig. 1).

2.2. Cytotoxic activity

The *in vitro* cytotoxic activity was evaluated for all of the synthesized compounds against the HepG2, BGC-823, SH-SY5Y, HeLa and HELF cell lines. Ursolic acid, paclitaxel and compounds **2**–**24** were dissolved in DMSO, dissolved in ethanol or diluted with culture medium containing 0.1% DMSO, respectively. The control cells were treated with culture medium containing 0.1% DMSO. Paclitaxel was used as a positive control. If 50% inhibition could not be reached at the highest concentration, then >100 μM was given. The results are shown in Table 1.

It can be seen from the IC_{50} values that ursolic acid suppressed proliferation of the above four cancer cell lines in different extents (IC_{50} values of 33.12–68.82 μM), and some modified compounds from it exhibited more effective, such as **11**, **13**–**16**, **21** and **23**. These derivatives showed similar inhibition activity against the HepG2, BGC-823 and SH-SY5Y cell lines, while the proliferation inhibition of HeLa cell lines was superior to other kinds of cancer cell lines.

The 3-OH of the modified ursolic acid derivatives was acetylated, resulting in 3-O-acetyl ursolic acids. When the 17-COOH was substituted by with a fatty alkyl group, the effect was significantly reduced as the length of the carbon chain was increased ($2 > 3 > 4$). Furthermore, the activity or even disappeared when the 3-OH and 17-COOH were both esterified (such as **8**–**10**), which suggested that keeping a polar group at either the 3-OH and/or 17-COOH position is essential for cytotoxic activity. On one hand, it may affect the hydrogen bonding, but on the other hand, the long chains may prevent cells from connecting with the mother nucleus.

NO-donating compounds **5**–**7** did not show significant anti-tumor activity as reported in the literature [12]. In our study, compound **5** had similar activity to UA, while compounds **6**–**7** showed decreased activity, which may be due to the same reasons as the long fatty alkyl group.

The previous study [10] showed that significant further improvement of cell growth inhibition was observed when an acetyl group was introduced at the 3-OH position and amino alkyl groups were introduced at the 17-COOH position. Similar results were seen in our study, where compounds **11** and **13**–**17** had more potent anti-tumor effects than compounds **18** and **20**–**24**, which had a free 3-OH group. Interestingly, compounds **12** and **19** were exceptions, exhibiting little antiproliferative effects, suggesting that

Table 1
The *in vitro* activity of **1**–**24** (expressed as IC_{50} (μM)) against HepG2, BGC-823, SH-SY5Y and HeLa human cancer cell lines, as well as the human embryonic lung fibroblast cell line HELF.[a]

Compoud	IC_{50} (μM)[a]				
	HepG2	BGC−823	SH-SY5Y	HeLa	HELF
1	68.82 ± 3.71	66.38 ± 0.66	54.62 ± 3.87	33.12 ± 0.63	21.28 ± 1.76
2	70.77 ± 3.88	69.32 ± 2.03	66.28 ± 0.45	29.18 ± 4.72	81.92 ± 3.19**
3	89.11 ± 4.02	79.68 ± 1.92	92.52 ± 3.22*	48.03 ± 2.98*	>100[b]
4	>100	>100	>100	63.24 ± 3.03**	>100
5	79.58 ± 0.45	84.24 ± 1.25	71.07 ± 2.35	36.21 ± 1.07	68.06 ± 2.11**
6	87.44 ± 2.10	98.28 ± 1.23*	89.57 ± 3.12*	69.39 ± 4.13**	82.56 ± 0.85**
7	>100	>100	>100	>100	>100
8	>100	>100	>100	>100	>100
9	>100	>100	>100	>100	>100
10	>100	>100	>100	>100	>100
11	35.26 ± 1.26**	29.01 ± 4.13**	37.18 ± 3.55**	20.61 ± 1.89*	22.34 ± 2.08
12	>100	82.95 ± 2.65	>100	66.97 ± 2.45**	35.81 ± 1.56*
13	46.62 ± 2.42*	48.47 ± 4.22	49.41 ± 1.34	16.27 ± 2.33	27.82 ± 1.56
14	20.25 ± 1.52**	15.52 ± 0.56**	13.24 ± 0.89**	10.87 ± 3.21**	38.06 ± 3.99
15	20.46 ± 2.53**	13.86 ± 2.45**	11.7 ± 1.08**	7.24 ± 3.11**	31.04 ± 2.13*
16	15.26 ± 4.10**	12.83 ± 2.30**	9.51 ± 0.45**	6.28 ± 0.88**	38.92 ± 2.43*
17	59.38 ± 0.42	51.34 ± 3.25	40.12 ± 2.13	12.43 ± 1.42	30.02 ± 2.03
18	83.03 ± 2.45	79.3 ± 2.14	72.21 ± 1.88	41.65 ± 1.45*	60.33 ± 1.22**
19	>100	>100	>100	>100	>100
20	82.36 ± 3.23*	78.26 ± 2.06	65.01 ± 2.96	32.33 ± 0.08*	52.75 ± 1.08**
21	35.66 ± 0.33*	39.27 ± 2.11*	21.38 ± 3.06*	14.36 ± 4.26*	36.92 ± 2.09*
22	>100	98.26 ± 2.06	>100	52.33 ± 0.08*	32.75 ± 1.08*
23	36.71 ± 1.36**	35.04 ± 2.03**	30.28 ± 2.56**	23.78 ± 3.19	28.06 ± 3.58
24	>100	>100	>100	67.29 ± 2.01	>100
Paclitaxol	10.32 ± 0.02**	9.24 ± 0.13**	8.56 ± 0.07**	6.62 ± 0.21**	7.17 ± 0.08*

Data are presented as mean ± SD ($n = 6$). *$P < 0.05$; **$P < 0.01$. compared with control.
[a] The concentration of the drug that inhibited cells growth by 50%.
[b] When 50% inhibition could not reached at the highest concentration, then >100 μM was given.

the introduction of a more bulky group (i.e., benzene ring) could increase the steric hindrance and decrease binding to the target.

The introduction of a diethanolamine structure at the 17-COOH position was done to determine whether a disubstituted amide structure was beneficial to the activity. Compounds **14** and **21** demonstrated better anticancer activities than ethanolamines **13** and **20**, in which the 3-OH group was free or acetylated, respectively.

The piperidine derivatives were relatively less active than the piperazidine, as the IC_{50} values showed, suggesting that the piperazine ring had better pharmacodynamic effects than the piperidine ring.

Considering the cytotoxicity of UA and its derivatives, the proliferation of HELF cells was tested. The activity of the UA ester compound decreased compared with UA. Among of the UA amide conjugates, those which possessed strong inhibition shared similar toxicity to UA, and certain modifications showed lower toxicity than UA (compounds **13, 14**, etc.).

Compound **14** showed significant activity against cancer cell lines (HepG2, C823, SH-SY5Y and HeLa) and lower cytotoxicity against HELF compared with ursolic acid (Fig. 2).

2.3. Investigation of apoptosis

It has been reported that UA induces apoptosis and growth inhibition at the G1 phase of the cell cycle in certain cancer cell systems [13]. Compound **14** was selected to analyze the mechanism of growth inhibition of HepG2 and BGC-823 cells by the following methods.

2.3.1. Fluorescence staining detection of cell apoptosis

The morphologic changes in the cell after treatment with compound **14** were assessed by fluorescence microscopy after staining with acridine orange (AO). Because AO can penetrate the normal cell membrane, the cells become stained uniformly to yield yellow-green fluorescence, while in apoptotic cells, apoptotic bodies are formed as a result of nuclear shrinkage, blebbing and broken fragments of different sizes. Therefore, staining showed intense green particles under a microscope (Fig. 3). With an increase in the concentration of the drug, this phenomenon was evident and the number of the apoptotic cells was increased, which suggested that compound **14** could induce cell apoptosis.

2.3.2. Annexin V-EGFP/PI apoptosis detection

Annexin V-EGFP/PI double staining kit was used to identify the cells in different states. HepG2 cells were double-labeled by Annexin V-EGFP/PI after they were treated with different concentrations of compound **14**; the control cells were treated with medium. The results are representative of three independent experiments. Four quadrant images were observed by flow cytometric analysis: the B1 area represented damaged cells appearing in the process of cell collection, the B2 region showed necrotic cells and later period apoptotic cells, the B3 area showed normal cells, and the early apoptotic cells were located in the B4 area. Our results (Fig. 4) showed that the early apoptotic cells were significantly more populous than in the untreated group and in a dose-dependent manner. In addition, necrosis and advanced apoptotic cells showed the same characteristics as the early apoptotic cells. The results illustrated that compound **14** suppressed cell proliferation by inducing apoptosis.

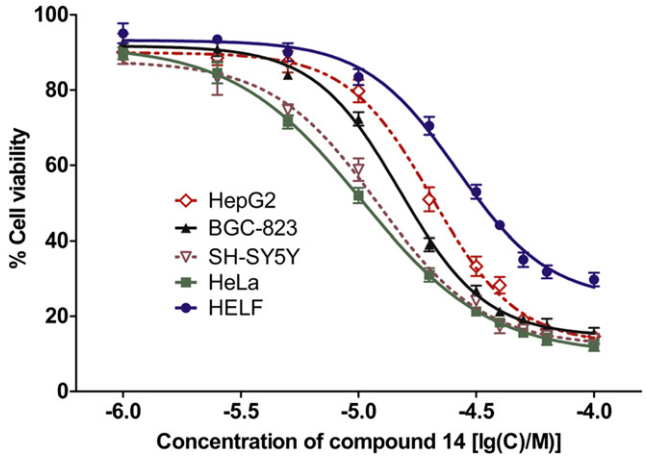

Fig. 2. Dose-response curves of the antiproliferative effect of compound 14 on HepG2, BGC-823, SH-SY5Y, HeLa and HELF cells.

2.3.3. Measurement of caspase-3 activity

The occurrence of the apoptotic process was confirmed by the presence of caspase-3 (which plays a crucial role and is a key element in the execution phase of apoptosis). The enzyme activity of caspase-3 was determined by spectrophotometry, as shown in Fig. 5. After incubation with compound **14** for 24 h, the activity of caspase-3 increased compared to the control. The results clearly showed that an induction of cell apoptosis took place when the cells were exposed to the drugs, and the derivative had better effect than UA based on the increased absorbance.

2.4. Investigation of cell cycle distribution

To determine the possible role of cell cycle arrest in UA derivative-induced growth inhibition, HepG2 cells were treated with different concentrations of compound **14**. Cell cycle distribution was observed by flow cytometric analysis after staining of the DNA with propidium iodide (PI). With an increase of concentration of compound **14**, the cells accumulated in the G0/G1 phase, and G2/M phase cells were gradually reduced, while S period cells were

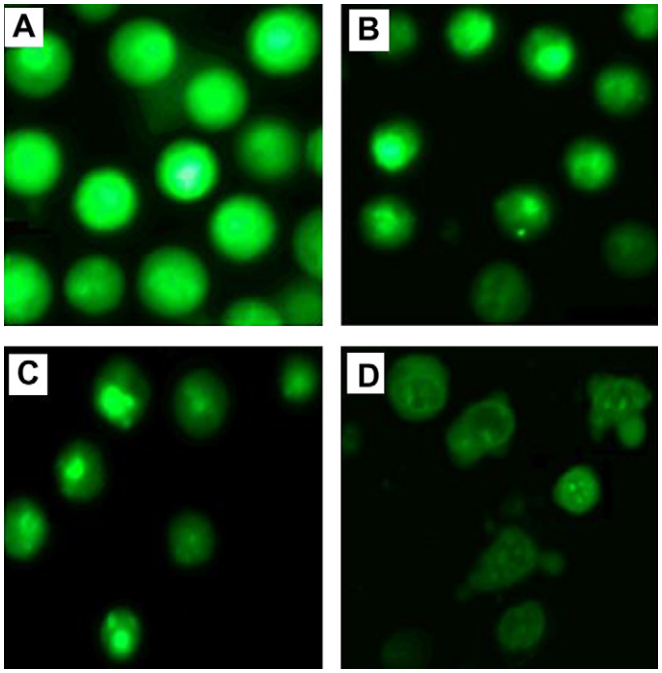

Fig. 3. Fluorescence images of acridine orange-stained HepG2 cells. Apoptotic cells were observed based on morphological changes in HepG2 cells after treatment with compound 14 at different concentrations 0 (control, A), 10 (B), 20 (C), 30 μM (D) for 24 h.(For interpretation of the references to colour in this figure legend, the reader is referred to the web version of this article.)

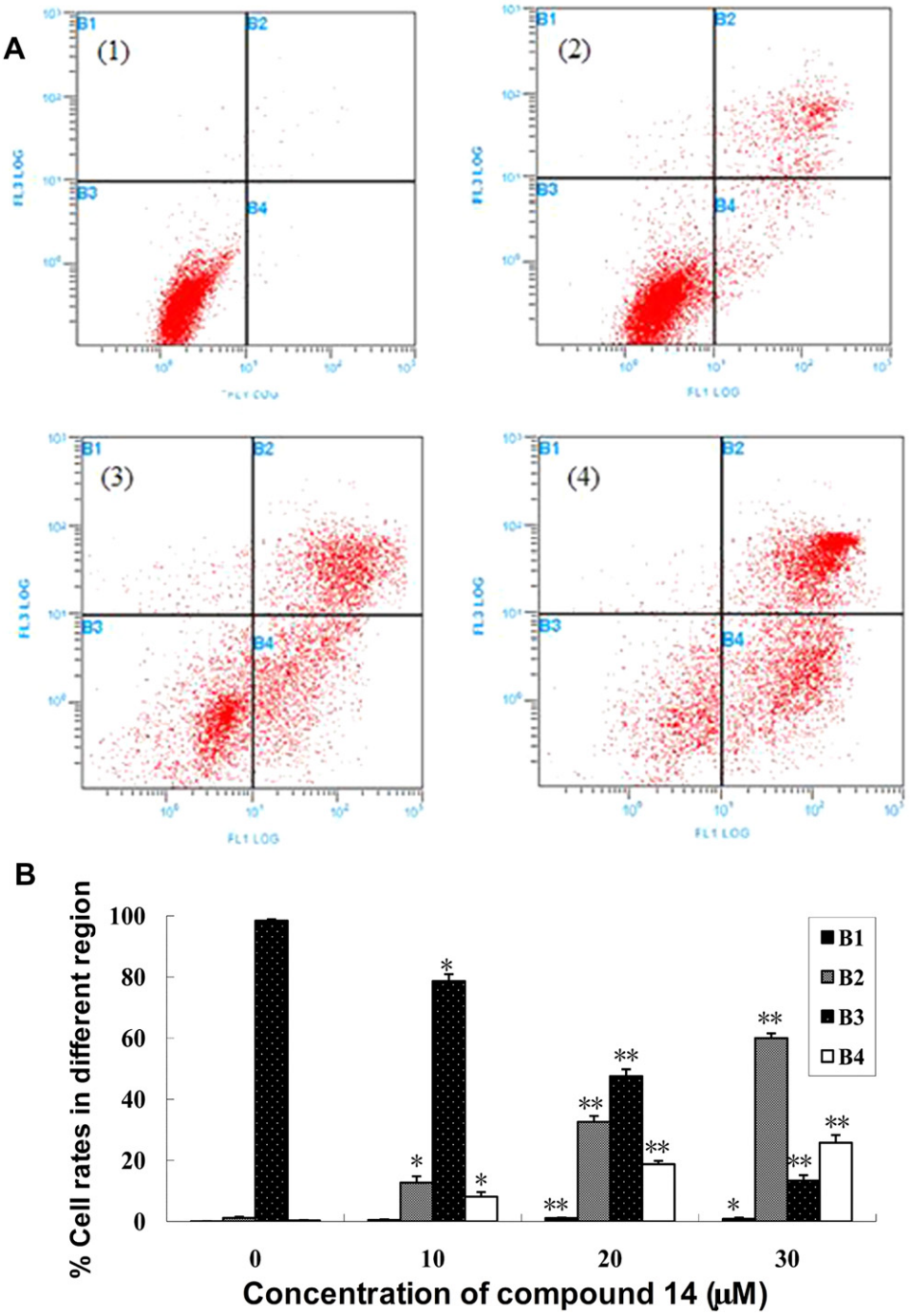

Fig. 4. Annexin V-EGFP/PI apoptosis detection assay. (A) Demonstration of apoptosis or necrosisby flow cytometric analysis. (1) Untreated HepG2 cells. (2)–(4) Cells were treated with increasing concentrations of compound 14 (10, 20 and 30 μM) for 24 h. (B) Dose-dependent induction of apoptosis or necrosisby compound 14. $^{*}P < 0.05$; $^{**}P < 0.01$, compared with control.

gradually increased (Fig. 6), which inferred that compound **14** arrested HepG2 cells in S phase.

2.5. Anti-tumorigenic activity of compound 14 against H22 xenograft tumor growth

Model Kunming mice bearing H22 hepatic carcinomas were established to observe the apoptosis of cells induced by UA and derivative compound **14** at different dosages. The medium dosage group (100 mg/kg) of compound **14** showed significant anticancer activity (45.6 ± 4.3%) as compared to the UA (150 mg/kg)-treated group (36.2 ± 3.6%) and cyclophosphamide (CTX)-treated group (55.0 ± 1.2%), even at the high dosage of 150 mg/kg (43.0 ± 2.6%) and low dosage of 150 mg/kg (36.6 ± 1.8%) (Fig. 7D). The body-weight of this group was also visibly increased (Fig. 7B). These data proved that compound **14** also exerted a preferable proliferation inhibition effect *in vivo*.

3. Conclusion

More and more studies have shown that ursolic acid has significant anti-tumor effects and exhibits cytotoxic activity

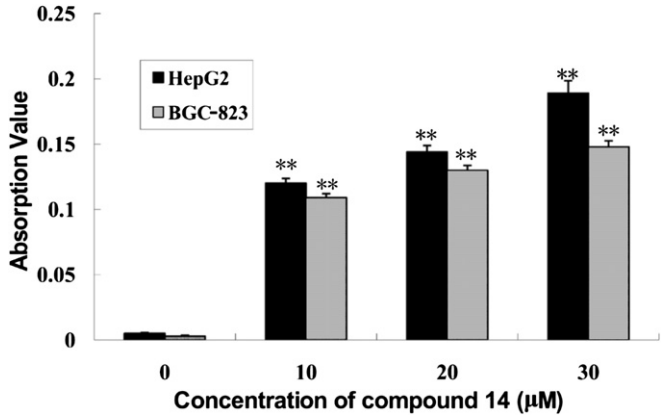

Fig. 5. Measurement of caspase-3 activity. Dose-dependent induction of caspase-3 in human HepG2 and BGC-823 cell lines. Data are mean ± SD ($n = 6$). $^{*}P < 0.05$; $^{**}P < 0.01$, compared with control.

against various kinds of cancer cell lines *in vitro*, which could be explained through the inhibition of DNA replication, activation of caspases, inhibition of protein tyrosine kinases and/or induction of Ca^{2+} release [14–16]. Another ursolic acid-induced apoptotic mechanism involves down-regulation of the cellular inhibitor of apoptosis gene [19] and the inhibition of NF-κB activity [20].

The above study results indicate that (1) ursolic acid can be modified to more potent bioactive derivatives. The 3-OH or 17-COOH esterified compounds showed decreasing inhibitory activity, and the effect was significantly reduced or even eliminated when they were esterified at the same time. Thus, keeping a polar group at either the 3-OH and/or 17-COOH position is essential for cytotoxic activity. (2) The inhibition effect of the ursolic acid ester compounds on the cancer cells decreases with increasing length of the carbon chain. We infer that long chains may prevent cells from connecting with the mother nucleus. (3) Significant improvement of the cell growth inhibition was achieved when an acetyl group was introduced at the 3-OH position and amino alkyl groups were introduced at the 17-COOH position. (4) The introduction of a more bulky group could increase the steric hindrance and decrease binding to the target. (5) A disubstituted amide structure is more likely to associate with the biomacromolecule through electrostatic interactions than monosubstituted amides. Moreover, a piperazine ring assumes a better position relative to a piperidine ring and improves activity. (6) Preliminary mechanistic studies demonstrated that compound **14** may inhibit cell growth by inducing apoptosis, arresting cell cycle progression at the S phase in HepG2 cells and increasing the activity of caspase-3. (7) The *in vivo* tests demonstrated that certain UA derivatives can provide better anti-tumor activity than UA. These findings can serve as the basis for further research on the chemical modifications, structure–activity relationships and bioactivity of UA and other triterpenoid acids.

4. Experimental

4.1. General

Ursolic acid was purchased from China Liuyang ATA Natural Product R&D Co., Ltd., in over 90% purity. Silica gel (200–300 mesh) used in column chromatography was provided by Tsingtao Marine Chemistry Co. Ltd. 3-O-acetylursolic acid was prepared according to a previous procedure [1]. Other reagents were obtained from commercial suppliers in analytically pure or chemically pure forms.

Melting points were determined on an electrically heated X-4 digital visual melting point apparatus and are uncorrected. IR spectra were recorded on Shimadzu FTIR-8400S. ^{1}H NMR spectra were recorded on a BRUKER AV-400 spectrometer with TMS as an internal standard in $CDCl_3$ or DMSO-d_6. Electrospray ionization (ESI) mass spectra were measured on an Agilent 1100 IC/MSD Trap XCT and are reported as *m/z*. Elemental analyses were recorded onVario Micro elemental analysis apparatus.

4.2. Synthesis

4.2.1. General procedure for the preparation of compounds (**8**–**10**)

3-O-acetylursolic acid (1 mmol) and K_2CO_3 (2 mmol) were added to DMF (30 mL) and stirred at room temperature for 4 h. The bromoalkane (4 mmol) was then dripped slowly into the mixture. After being stirred for another 8 h, the reaction mixture was poured into the 100 mL distilled water and partitioned with ethyl acetate (3 × 50 mL). The organic layer was washed with saturated sodium chloride, dried over Na_2SO_4, and purified via silica gel column chromatography with petroleum ether/ethyl acetate.

*4.2.1.1. 3β-Acetoxy-urs-12-en-28-oic acid ethyl ester (**8**).* According to the general procedure, 3-O-acetylursolic acid was treated with bromoethane, and then purified on silica gel column using petroleum ether/ethyl acetate (v/v 10:1) as eluent to give compound **8** ($R_f = 0.59$).

Yield: 87.29%; white powder; mp: 177–180 °C; IR (KBr) υ: 2927, 1735, 1718, 1455, 1374, 1250, 1028 cm^{-1}; ^{1}H NMR (400 MHz, $CDCl_3$) δ: 5.23 (t, $J = 3.6$ Hz, 1 H, H-12), 4.49 (dd, $J = 7.2$, 10.0 Hz, 1 H, H-3), 4.04 (q, $J = 6.4$ Hz, 2 H, CH_2), 2.22 (d, $J = 11.6$ Hz, 1 H, H-18), 2.03 (s, 3 H, CH_3COO), 1.24 (t, $J = 7.6$ Hz, 3 H, CH_2CH_3), 1.07 (s, 3 H, CH_3), 0.98 (s, 3 H, CH_3), 0.94–0.91 (s, 6 H, 2 × CH_3), 0.84–0.78 (m, 9 H, 3 × CH_3), 0.76 (s, 3 H, CH_3); ESI-MS *m/z*: 527.6 $(M + H)^+$; Anal. Calcd for $C_{34}H_{54}O_4$: C 77.52, H 10.33; Found: C 77.41, H 10.27.

*4.2.1.2. 3β-Acetoxy-urs-12-en-28-oic acid propyl ester (**9**).* According to general procedure, 3-O-acetylursolic acid was treated with 1-bromopropane, and then purified on silica gel column using petroleum ether/ethyl acetate (v/v 10:1) as eluent to afford compound **9** ($R_f = 0.57$).

Yield: 85.31%; amorphous powder; mp: 175–176 °C; IR (KBr) υ: 2948, 1736, 1722, 1456, 1374, 1257, 1028 cm^{-1}; ^{1}H NMR (400 MHz, $CDCl_3$) δ: 5.23 (t, $J = 3.4$ Hz, 1 H, H-12), 4.49 (t, $J = 7.6$ Hz, 1 H, H-3), 3.73–3.69 (m, 2 H, $COOCH_2$), 2.29 (d, $J = 10.6$ Hz, 1 H, H-18), 2.16–2.07 (m, 2 H, CH_2CH_2), 1.43–1.24 (m, 6 H, 2 × CH_3), 0.99–0.94 (m, 9 H, 3 × CH_3), 0.83 (d, 3 H, CH_3), 0.77 (s, 3 H, CH_3), 0.75 (s, 3 H, CH_3); ESI-MS *m/z*: 541.6 $(M + H)^+$; Anal. Calcd for $C_{35}H_{56}O_4$: C 77.73, H 10.44; Found: C 77.44, H 10.37.

*4.2.1.3. 3β-Acetoxy-urs-12-en-28-oic acid n-butyl ester (**10**).* According to the general procedure, 3-O-acetylursolic acid was treated with n-butyl bromide, and then purified on silica gel column using petroleum ether/ethyl acetate (v/v 10:1) as eluent to obtain compound **10** ($R_f = 0.56$).

Yield: 86.57%; amorphous powder; mp: 107–109 °C; IR (KBr) υ: 2941, 1735, 1716, 1455, 1372, 1244, 1027 cm^{-1}; ^{1}H NMR (400 MHz, $CDCl_3$) δ: 5.22 (t, $J = 3.4$ Hz, 1 H, H-12), 4.48 (t, $J = 7.8$ Hz, 1 H, H-3), 4.05–3.99 (m, 2 H, $COOCH_2$), 2.22 (d, $J = 11.2$ Hz, 1 H, H-18), 2.03 (s, 3 H, CH_3COO), 2.00–1.94 (m, 2 H, CH_2CH_2), 1.60–1.55 (m, 2 H, CH_2CH_2), 1.43–1.19 (m, 12 H, 4 × CH_3), 1.08 (s, 3 H, CH_3), 0.98–0.82 (m, 6 H, 2 × CH_3), 0.76 (s, 3 H, CH_3); ESI-MS *m/z*: 555.6 $(M + H)^+$; Anal. Calcd for $C_{36}H_{58}O_4$: C 77.93, H 10.54; Found: C 77.67, H 10.49.

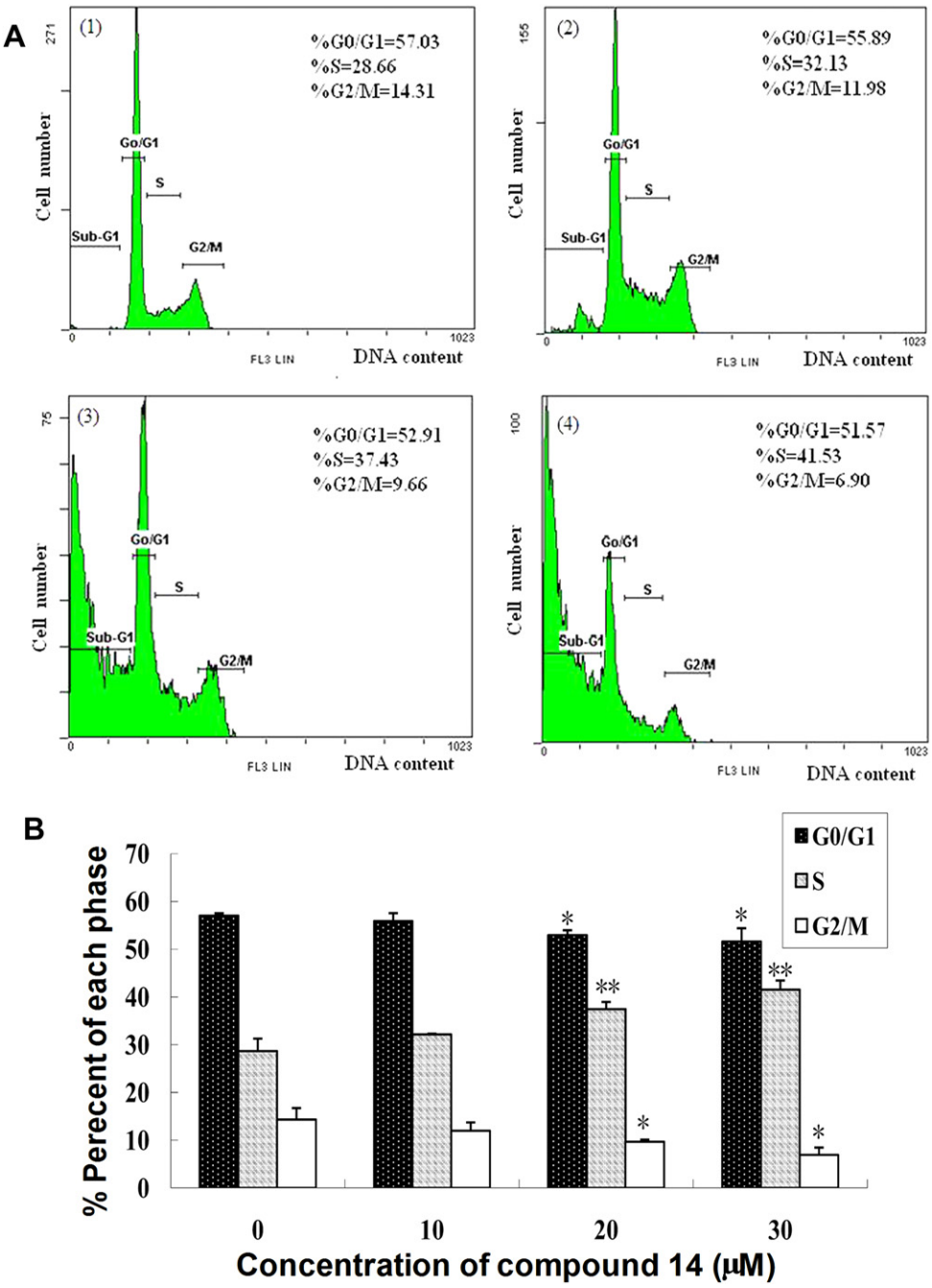

Fig. 6. Investigation of cell cycle distribution. (A) Demonstration of apoptosis by flow cytometric analysis. (1) Untreated HepG2 cells. (2)–(4) Cells was treated with increasing concentrations of compound 14 (10, 20 and 30 μM) for 24 h. (B) Dose-dependent induction of apoptosis by compound 14. $^{*}P < 0.05$; $^{**}P < 0.01$, compared with control.

*4.2.2. General procedure for the preparation of N-[3β-acetoxy-urs-12-en-28-oyl]-amino acid methyl-esters, alkamines, piperazidines, piperidine (**14**–**17**)*

Oxalyl chloride (0.6 mL) was added in three equal portions to a CH_2Cl_2 solution of (insert the related compound number) (1 mmol) and stirred at room temperature for 36 h. The mixture was concentrated to dryness under reduced pressure to obtain crude 3-O-acetylursolyl chloride. This intermediate was dissolved in a CH_2Cl_2 (20 mL) solution, and then treated with amino acid methyl-ester, alkamines, piperazidines or piperidine. The mixture was stirred at room temperature for 4 h and treated with triethylamine until the pH was 8–9. Next, the mixture was concentrated to dryness. The residue was partitioned in 10 mL water and adjusted with 2 N HCl to pH 3–4 and filtered. The crude material was purified on a silica gel column with the appropriate eluent to yield compounds **14**–**17**.

*4.2.2.1. N-[3β-acetoxy-urs-12-en-28-oyl]-2-aminodiethanol (**14**).* According to the general procedure, 3-O-acetylursolic acid was treated with diethanolamine, and then purified on silica gel column using petroleum ether/ethyl acetate (v/v 1:3) as eluent to give compound **14** ($R_f = 0.53$).

Yield: 50.37%; white powder; mp: 226–228 °C; IR (KBr) υ: 3392, 2946, 1734, 1595, 1371, 1245 cm^{-1}; ^1H NMR (400 MHz, DMSO-d_6) δ: 5.08 (t, $J = 3.6$ Hz, 1 H, H-12), 4.42 (t, $J = 6.8$ Hz, 1 H, H-3), 3.42 (t, $J = 9.2$ Hz, 2 H, N ($\underline{CH_2}$)$_2$), 2.33 (t, $J = 6.8$ Hz, 1 H, $CH_2\underline{CH_2}$), 2.00 (s, 3 H, $C\underline{H_3}COO$), 1.04 (s, 3 H, CH_3), 0.91–0.90 (m, 6 H, 2 × CH_3),

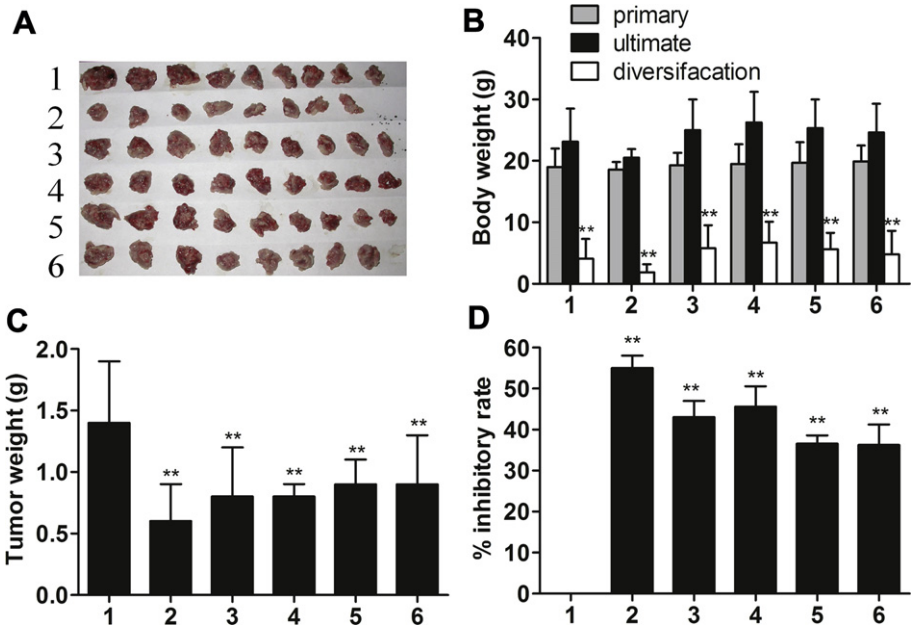

Fig. 7. Effect of anti-tumor *in vivo*. H22 tumor-bearing mice were administered i.p. 7 days with normal saline (1) CTX at 15 mg/kg (2) compound 14 at 50, 100 and 150 mg/kg (3–5) UA at 150 mg/kg (6) The figure shows the tumor mode (A) and body weight (B) of the control and therapeutic groups. (C) shows the tumor weight and (D) shows the inhibitory rates after administration. Data represent means ± S.D. from three independent experiments performed in duplicate. $^{*}P < 0.05$; $^{**}P < 0.01$ vs. the normal saline (1).

0.83–0.81 (m, 9 H, 3 × CH_3), 0.70 (s, 3 H, CH_3); ESI-MS *m/z*: 586.9 $(M + H)^+$; Anal. Calcd for $C_{36}H_{59}NO_5$: C 73.8, H 10.15, N 2.39; Found: C 73.59, H 10.11, N 1.98.

*4.2.2.2. N-[3β-acetoxy-urs-12-en-28-oyl]-amino-N- (2-hydroxyethyl) piperazine (**15**).* According to the general procedure, 3-O-acetylursolic acid was treated with *N*- (2-Hydroxyethyl) piperazine, and then purified on silica gel column using chloroform/acetone (v/v 3:1) to give compound **15** ($R_f = 0.43$).

Yield: 46.81%; white powder; mp: 196–198 °C; IR (KBr) υ: 3417, 2943, 1724, 1595, 1368, 1251 cm^{-1}; ^1H NMR (400 MHz, $CDCl_3$) δ: 5.22 (s, 1 H, H-12), 4.48 (t, *J* = 6.0 Hz, 1 H, H-3), 3.63 (t, *J* = 5.2 Hz, 2 H, $C\underline{H}_2OH$), 3.22 (t, *J* = 3.2 Hz, 1 H, H-3), 2.55 (t, *J* = 5.2 Hz, 2 H, -N $(C\underline{H}_2)_2$), 2.47 (br, 4 H, -N $(CH_2C\underline{H}_2)_2$), 2.04 (s, 3 H, $C\underline{H}_3CO$), 1.07 (s, 3 H, $C\underline{H}_3$), 0.95 (s, 3 H, CH_3), 0.93 (d, *J* = 6.4 Hz, 3 H, $CH\underline{CH}_3$), 0.91 (s, 3 H, CH_3), 0.86 (d, *J* = 6.4 Hz, 3 H, CH_3), 0.85 (s, 3 H, CH_3), 0.75 (s, 3 H, CH_3); LC-MS *m/z* 611.6 $(M + H)^+$, 633.6 $(M + Na)^+$; Anal. Calcd for $C_{38}H_{62}N_2O_4$: C 74.71, H 10.23, N 4.59; Found: C 74.66, H 10.16, N 4.08.

*4.2.2.3. N-[3β-acetoxy-urs-12-en-28-oyl]-amino-1-hydroxyethylethoxy piperazine (**16**).* According to the general procedure, treatment of 3-O-acetylursolic acid with 1-hydroxyethylethoxy piperazine, and then purified on silica gel column using chloroform/acetone (v/v 3:1) afforded compound **16** ($R_f = 0.36$).

Yield: 37.87%; white powder; mp: 105–107 °C; IR (KBr) υ: 3446, 2945, 1734, 1633, 1370, 1246 cm^{-1}; ^1H NMR (400 MHz, $CDCl_3$) δ: 5.21 (s, 1 H, H-12), 4.48 (t, *J* = 4.0 Hz, 1 H, H-3), 3.71–3.61 (m, 8 H, 4 × $C\underline{H}_2$), 2.58 (t, *J* = 5.2 Hz, 2 H, -N $(C\underline{H}_2)_2$), 2.48 (br, 4 H, -N $(CH_2C\underline{H}_2)_2$), 2.04 (s, 3 H, $C\underline{H}_3CO$), 1.06 (s, 3 H, CH_3), 0.93 (d, *J* = 6.0 Hz, 3 H, CH_3), 0.86–0.84 (m, 9 H, 3 × CH_3), 0.84 (s, 3 H, CH_3), 0.73 (s, 3 H, CH_3); LC-MS *m/z* 656.1 $(M + H)^+$, 677.6 $(M + Na)^+$; Anal. Calcd for $C_{40}H_{66}N_2O_5 \cdot H_2O$: C 73.35 (71.39), H 10.16 (9.89), N 4.28 (4.17); Found: C 71.86, H 10.03, N 3.74.

*4.2.2.4. N-[3β-acetoxy-urs-12-en-28-oyl]-amino-4-piperidineethanol (**17**).* According to the general procedure, treatment of 3-O-acetylursolic acid with 4-piperidineethanol, and then purified on silica gel column using chloroform/acetone (v/v 3:1) afforded compound **17** ($R_f = 0.61$).

Yield: 58.72%; white powder; mp: 138–140 °C; IR (KBr) υ:3409, 2943, 1728, 1585, 1367, 1253 cm^{-1}; ^1H NMR (400 MHz, $CDCl_3$) δ: 5.22 (s, 1 H, H-12), 4.48 (d, *J* = 4.0 Hz, 1 H, H-3), 4.37 (t, *J* = 6.4 Hz, 2 H, $C\underline{H}_2OH$), 3.72–3.70 (m, 2 H, $C\underline{H}_2CH_2OH$), 2.73–2.70 (m, 4 H, -N-$(C\underline{H}_2)_2$), 2.43 (s, 3 H, CH_3COO), 2.04 (d, *J* = 3.6 Hz, 1 H, H-18), 1.51–1.49 (m, 1 H, $(CH_2)_3$-C<u>H</u>-), 1.30–1.27 (m, 4 H, -N $(CH_2C\underline{H}_2)_2CH$-), 1.07 (s, 3 H, CH_3), 0.94 (s, 3 H, CH_3), 0.86–0.85 (m, 12 H, 4 × CH_3), 0.76 (s, 3 H, CH_3); LC-MS *m/z* 610.6 $(M + H)^+$, 632.6 $(M + Na)^+$; Anal. Calcd for $C_{39}H_{63}NO_4$: C 76.8, H 10.41, N 4.28; Found: C 76.75, H 10.32, N 4.21.

*4.2.3. General procedure for the synthesis of N-[3β-hydroxy-urs-12-en-28-oyl]- amino acids alkamines, piperazidines, piperidine (**22**–**24**)*

A solution of **15**–**17** in aqueous NaOH (4 N) in CH_3OH:THF (1:1.5, v: v) was stirred for 4 h at room temperature and concentrated under reduced pressure. The residue was suspended in water, adjusted with 2 N HCl to pH 3–4 and then filtered. The filter was washed with water to pH 6–7, and the material was dried to obtain compounds **22**–**24**.

*4.2.3.1. Synthesis of N-[3β-hydroxy-12-en-28-oyl]-amino-N- (2-Hydroxyethyl)piperazine (**22**).* According to the general procedure, compound **22** was obtained by hydrolysis of compound **15**. R_f [chloroform/acetone (v/v 4:1)] = 0.29.

Yield: 81.38%; mp: 208–210 °C; IR (KBr) υ: 3380, 2926, 1635, 1368 cm^{-1}; ^1H NMR (400 MHz, $CDCl_3$) δ: 5.22 (s, 1 H, H-12), 3.63 (t, *J* = 6.0 Hz, 2 H, $C\underline{H}_2OH$), 3.22 (t, *J* = 3.2 Hz, 1 H, H-3), 2.55 (t, *J* = 5.2 Hz, 2 H, -N $(C\underline{H}_2)_2$), 2.47 (br, 4 H, -N $(CH_2C\underline{H}_2)_2$), 2.17 (t, *J* = 3.6 Hz, 1 H, H-18), 1.07 (s, 3 H, CH_3), 0.98 (s, 3 H, CH_3), 0.94 (d, *J* = 6.0 Hz, 3 H, CH_3), 0.91 (s, 3 H, CH_3), 0.87 (d, *J* = 6.4 Hz, 3 H, CH_3), 0.77 (s, 3 H, CH_3), 0.75 (s, 3 H, CH_3); LC-MS *m/z* 570.0 $(M + H)^+$, 591.5 $(M + Na)^+$; Anal. Calcd for $C_{36}H_{60}N_2O_3$: C 76.01, H 10.63, N 4.92; Found: C 75.59, H 10.59, N 4.81.

*4.2.3.2. N-[3β-acetoxy-urs-12-en-28-oyl]-amino-1-hydroxyethylethoxypiperazine (**23**).* According the general procedure, compound **23** was obtained by hydrolysis of compound **16**. R_f [chloroform/acetone (v/v 4:1)] = 0.27.

Yield: 87.26%; mp: 111–113 °C; IR (KBr) υ: 3414, 2925, 1616, 1376, 1227 cm^{-1}; ^1H NMR (400 MHz, $CDCl_3$) δ: 5.21 (s, 1 H, H-12), 3.71 (t, J = 4.4 Hz, 2 H, $C\underline{H}_2CH_2OH$), 3.71–3.61 (m, 8 H, 4 × $C\underline{H}_2$), 2.58 (t, J = 5.2 Hz, 4 H, -N $(C\underline{H}_2)_2$), 2.49 (br, 4 H, -N $(CH_2C\underline{H}_2)_2$), 1.05 (s, 3 H, CH_3), 0.94–0.93 (m, 6 H, 2 × CH_3), 0.88–0.85 (m, 9 H, 3 × CH_3), 0.76 (s, 3 H, CH_3); LC-MS m/z 613.6 $(M + H)^+$, 635.6 $(M + Na)^+$; Anal. Calcd for $C_{38}H_{64}N_2O_4$: C 74.46, H 10.52, N 4.57; Found: C 74.21, H 10.44, N 4.41.

*4.2.3.3. N-[3β-acetoxy-urs-12-en-28-oyl]-amino-4-piperidineethanol (**24**).* According the general procedure, compound **24** was obtained by hydrolysis of compound **17**. R_f [chloroform/acetone (v/v 8:1)] = 0.34.

Yield: 89.32%; mp:201–203 °C; IR (KBr) υ: 3426, 2926, 1610, 1369, 1270 cm^{-1}; ^1H NMR (400 MHz, $CDCl_3$) δ: 5.22 (s, 1 H, H-12), 4.37–4.35 (m, 2 H, $C\underline{H}_2CH_2OH$), 3.71 (t, J = 6.0 Hz, 2 H, $C\underline{H}_2OH$), 3.21 (t, J = 3.2 Hz, 1 H, H-3), 2.76–2.71 (m, 4 H, -N- $(C\underline{H}_2)_2$), 2.18 (t, J = 10.8 Hz, 1 H, H-18), 1.54–1.49 (m, 1 H, $(CH_2)_3$-$C\underline{H}$-), 1.31–1.25 (m, 4 H, -N $(CH_2C\underline{H}_2)_2CH$-), 1.07 (s, 3 H, CH_3), 0.98 (s, 3 H, CH_3), 0.94 (d, J = 6.0 Hz, 3 H, CH_3), 0.91 (s, 3 H, CH_3), 0.87 (d, J = 6.4 Hz, 3 H, CH_3), 0.78 (s, 3 H, CH_3), 0.76 (s, 3 H, CH_3); LC-MS m/z 568.6 $(M + H)^+$, 590.6 $(M + Na)^+$; Anal. Calcd for $C_{37}H_{61}NO_3$: C 78.25, H 10.83, N 2.47; Found: C 78.01, H 10.79, N 2.32.

4.3. Single crystal X-ray diffraction

Single crystal X-ray diffraction experiment was performed on Rigaku Saturn-724, equipped with graphite-monochromated Mo-Kα radiation (λ = 0.71073 Å) at room temperature. The structures were solved by direct methods and refined on F2 by full-matrix least-squares methods using the SHELXTL-97 program package. All non-hydrogen atom positions were located using difference Fourier methods as implemented in SHELXL-97. All H atoms were placed in calculated positions on their corresponding O and C atoms.

4.4. Cell lines and culture

HepG2, BGC-823, SH-SY5Y, HeLa and HELF cells were all obtained from our own laboratory. They were maintained in RPMI 1640 medium supplemented with 10% FBS, penicillin (100 U/mL), and streptomycin (100 μg/mL) in a humidified atmosphere of 5.0% CO_2 at 37 °C.

4.5. MTT assay for cell viability/proliferation

The cytotoxicity of the derivatives was determined by the MTT assay. Cells (1 × 10^4/well) were plated in 100 μL of medium/well in 96-well plates. After incubation overnight, the cells were treated with different concentrations of drugs in RPMI 1640 with 10% FBS for 24 h. Finally, MTT was added, and the cells were incubated for another 4 h. The MTT-formazan formed by metabolically viable cells was dissolved in 150 mL of DMSO and shaken for 10 min. The absorbance was then measured on an ELISA reader at a test wavelength of 490 nm. Each test was repeated at least three times. The concentration of the compound, which gives the 50% growth inhibition value, corresponds to the IC_{50}.

4.6. Apoptosis tests

4.6.1. Morphologic evaluation by fluorescence microscopy

Cells incubated with different concentrations of compound **14** (10–30 μM) for 24 h were collected, washed with PBS and suspended in solution at a cell density of 1 × 10^6/mL. Then, 95 μL of cell suspension was stained with 5 μL (200 μg/mL in PBS) of AO for 15 min at room temperature in the dark. Stained cells were visualized with a Nikon fluorescence microscope using a 488 nm excitation while measuring fluorescence at 515 nm.

4.6.2. Annexin V-EGFP/PI double staining

Cells in different states were observed with an annexin V-EGFP/PI double staining kit. HepG2 cells were treated with different concentrations of compound **14** (10–30 μM) for 24 h. After incubation, a total of 3 × 10^5 cells were harvested from the treated and normal samples. The cells were washed twice with PBS, and then 5 μL of annexin V-EGFP and propidiumiodide (PI) were added in the dark for 15 min. The cells were then analyzed by analytical flow cytometry using a Cell Lab Quanta SC (Beckman, USA). All experiments were performed three times.

4.6.3. Caspase-3 enzyme assay

The activity of the caspase-3 protein was determined following the test kit instructions (R&D Systems, Inc.). Twenty-four hours after culturing, 5 × 10^5–10^6 cells were collected, washed twice with PBS and centrifuged at 500 g for 5 min. Then, 25 μL of lysis buffer was added to the cells on ice for 10 min, and then 50 μL of 2 × reaction buffer 3 and 5 μL of caspase-3 substrate (DEVD-pNA) were added. After incubating at 37 °C for 1–2 h in darkness, the absorbance was measured at 405 nm, with the lysis buffer and reactionbuffer (25 μL lysis buffer + 50 μL 2 × reaction buffer) as control.

4.7. Cell cycle assay

The cell cycle was analyzed by flow cytometry. Briefly, HepG2 cells were treated with different concentrations of compound **14** (10–30 μM) for 24 h. After incubation, a total of 1 × 10^8 cells were harvested from the treated and normal samples. The cells were washed twice with PBS and fixed in 75% ice-cold ethanol for at least overnight. The sample was concentrated by removing the ethanol and staining the cellular DNA with fluorescent solution (1% (v/v) Triton X-100, 0.01% RNase, 0.05% PI) for 30 min at 4 °C in darkness. The cell cycle distribution was then detected by flow cytometry. All experiments were performed three times.

4.8. Evaluation of therapeutic effect in vivo

Kunming mice (16–19 g body weight, 6–8 weeks old) were maintained under identical laboratory conditions and given standard food pellets and water ad libitum. After inoculation with murine hepatoma H22 cells for 24 h, tumor-bearing mice were randomized into six experimental groups, each with 10 mice. All compounds were dissolved in 10% DMSO solution. Group I was the negative control (normal saline) and group II was the positive control (CTX; 1.5 mg/mL). Group III-VI was treated with 20, 40 or 60 μM compound **14** and UA (60 μM), respectively. All of the compounds were administered at a dose of 0.2 ml/10 g bodyweight for seven successive days. At the end of the experiment, the animals were sacrificed and the tumors were dissected and weighed. The tumor inhibitory rates were then calculated.

4.9. Statistical analysis

The data were presented as means ± standard deviations of three determinations. Statistical analysis was performed using Student's *t*-test and one-way analysis of variance. Multiple comparisons of the means were done by the least significance difference (LSD) test. A probability value of <0.05 was considered

significant. All computations were made by employing SPSS statistical software (version 16.0).

Acknowledgments

This research was supported by grants from the Creation Platform Project of the Young Scientist Innovation Foundation of Fujian Province of China (No.2007F0347), Scientific and Technological Foundation of Fujian Province of China (No.JA08004) and Scientific and Technological Foundation of Fuzhou University (No.826804).

Appendix. Supplementary data

Supplementary data associated with this article can be found in online version at doi:10.1016/j.ejmech.2011.03.050.

References

[1] C.M. Ma, N. Nakamura, M. Hattori, H. Kakuda, J.C. Qiao, H.L. Yu, Inhibitory effects on HIV-1 protease of constituents from the wood of Xanthoceras sorbifolia, J. Nat. Prod. 63 (2000) 238–242.
[2] B. Saraswat, P.K. Visen, D.P. Agarwal, Ursolic acid isolated from Eucaliptus tereticornis protects against ethanol toxicity in isolated rat hepatocytes, Phytother. Res. 14 (2000) 163–166.
[3] F. Traore-Keita, M. Gasquet, C. Di Giorgio, E. Ollivier, F. Delmas, A. Keita, O. Doumbo, G. Balansard, P. Timon-David, Antimalarial activity of four plants used in traditional medicine in Mali, Phytother. Res. 14 (2000) 45–47.
[4] D. Chattopadhyay, G. Arunachalam, A.B. Mandal, T.K. Sur, S.C. Mandal, S.K. Bhattacharya, Antimicrobial and antiinflammatory activity of folklore Mallotus peltatus: leaf extract, J. Ethnopharmacol. 82 (2002) 229–237.
[5] J. Li, W.J. Guo, Q.Y. Yang, Effects of ursolic acid and oleanolic acid on human colon carcinoma cell line HCT15, World J. Gastroenterol. 8 (2002) 493–495.
[6] D. Anderson, J.J. Liu, A. Nilsson, Ursolic acid inhibits proliferation and stimulates apoptosis in HT29 cells following activation of alkaline sphingomyelinase, Anticancer Res. 23 (2003) 3317–3322.
[7] Y.H. Choi, J.H. Baek, M.A. Yoo, H.Y. Chung, N.D. Kim, K.W. Kim, Induction of apoptosis by ursolic acid through activation of caspases and down-regulation of c-IAPs in human prostate epithelial cells, Int. J. Oncol. 17 (2000) 565–570.
[8] H.Y. Tu, A.M. Huang, B.L. Wei, K.H. Gan, T.C. Hour, S.C. Yang, Y.S. Pu, C.N. Lin, Ursolic acid derivatives induce cell cycle arrest and apoptosis in NTUB1 cells associated with reactive oxygen species, Bioorg. Med. Chem. 17 (2009) 7265–7274.
[9] Y. Kashiwada, T. Nagao, A. Hashimoto, Y. Ikeshiro, H. Okabe, L.M. Cosentino, K.H. Lee, Anti-AIDS agents 38. Anti-HIV activity of 3-O-acyl ursolic acid derivatives, J. Nat. Prod. 63 (2000) 1619–1622.
[10] Y.Q. Meng, D. Liu, L.L. Cai, The synthesis of ursolic acid derivatives with cytotoxic activity and the investigation of their preliminary mechanism of action, Bioorg. Med. Chem. 17 (2009) 848–854.
[11] C.M. Ma, S.Q. Cai, J.R. Cui, R.Q. Wang, P.F. Tu, H. Masao, D. Mohsen, The cytotoxic activity of ursolic acid derivatives, Eur. J. Med. Chem. 40 (2005) 582–589.
[12] D.K. Kim, J.H. Baek, C.M. Kang, M.A. Yoo, J.W. Sung, H.Y. Chung, N.D. Kim, Y.H. Choi, S.H. Lee, K.W. Kim, Apoptotic activity of ursolic acid may correlate with the inhibition of initiation of DNA replication, Int. J. Cancer 87 (2000) 629–636.
[13] H.J. Heo, H.Y. Cho, B. Hong, H.K. Kim, T.R. Heo, E.K. Kim, S.K. Kim, C.J. Kim, D.H. Shin, Ursolic acid of Origanum majorana L. reduces abeta-induced oxidative injury, Mol. Cell. 13 (2002) 5–11.
[14] F. Lauthier, L. Taillet, P. Trouillas, C. Delag, A. Simon, Ursolic acid triggers calcium-dependent apoptosis in human Daudi cells, Anticancer Drugs 11 (2000) 737–745.
[15] P.O. Harmand, R. Duval, B. Liagre, C. Jayat-Vignoles, J.L. Beneytout, C. Delage, A. Simon, Ursolic acid induces apoptosis through caspase-3 activation and cell cycle arrest in HaCat cells, Int. J. Oncol. 23 (2003) 105–112.
[16] S. Shishodia, S. Majumdar, S. Banerjee, B.B. Aggarwal, Ursolic acid inhibits nuclear factor-kappaB activation induced by carcinogenic agents through suppression of IkappaB alpha kinase and p65 p.osphorylation: correlation with down-regulation of cyclooxygenase 2, matrix metalloproteinase 9, and cyclin D1, Cancer Res. 63 (2003) 4375–4383.